

Pion-Pion Interactions in π^+p Collisions*

D. L. STONEHILL[†] AND H. L. KRAYBILL

Yale University, New Haven, Connecticut

THEORETICAL and experimental evidence for direct pion-pion interactions has been accumulating steadily during the past few years. The large pion-proton interaction radius of about 1 F, indicated by large total cross sections persisting up to energies of several BeV and higher,¹ suggests directly that the incident pion interacts with the meson cloud rather than the bare core of the proton. Theoretical analysis² of electron-proton scattering predicts a pion-pion resonance with $T = 1$, $J = 1$, at a somewhat uncertain energy. Pion-pion resonances with $T = 0$ have also been predicted.³ During 1960, several laboratories reported indications of resonances at various energies.⁴ Early in 1961, a rise was reported in the $\pi^+\pi^0$ cross section up to about 700 MeV,⁵ and evidence for a resonance at about 760 MeV was reported by Erwin *et al.*⁶ Its existence has been confirmed by several other laboratories⁷⁻⁹ and it has been named the " ρ " meson. Since then, two other energy-dependent pion-pion interactions (ω, η) have been discovered,⁹⁻¹¹ and the possible existence of another (ζ) has

been reported.¹² Their properties are summarized in Table I.

TABLE I. Energy-dependent pion-pion interactions.

Name	Mass (MeV)	Width (Γ) ^a (MeV)	I -spin	Decay	Probable j
Rho	760	~ 100	1	2 pi	1
Omega	790	< 25	0	3 pi	1
Eta	550	< 15	0	3 pi	?
Zeta (?)	575	?	1	2 pi	?

^a Full width at half-maximum.

During the past year, we have been studying the occurrence of pion-pion interactions in collisions of positive pions with protons, at incident pion kinetic energies of 910, 1090, and 1260 MeV. Identification and kinematical analysis of 8500 two-prong π^+p interactions at these energies in the Brookhaven 20-in. hydrogen bubble chamber has been completed. Table II shows the classification of these events by energy and by reaction products.

The reactions of principal interest for pion-pion interaction are those producing a single pion: $\pi^+ + p \rightarrow p + \pi^+ + \pi^0$, and $\pi^+ + p \rightarrow n + \pi^+ + \pi^+$. The simplest pion-pion mechanism is indicated in Fig. 1,

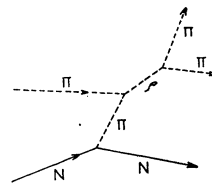


FIG. 1. Simplest pion-pion interaction diagram for pion-nucleon collisions. N is the target nucleon, N' the recoil nucleon.

in which the incident pion interacts with a virtual meson emitted by the proton. This mechanism has a higher probability of producing small four-momen-

* This work was partially supported by the U. S. Atomic Energy Commission.

[†] Part of the work reported here has been included in a thesis which will be submitted by D. L. Stonehill in partial fulfillment of requirements for the Ph.D. degree at Yale University.

¹ G. Maechen, W. B. Fowler, W. M. Powell, and R. W. Wright, *Phys. Rev.*, **103**, 850 (1957); W. D. Walker, *ibid.*, **103**, 872 (1957); C. Goebel, *Phys. Rev. Letters* **1**, 337 (1958).

² W. R. Frazer and J. R. Fulco, *Phys. Rev. Letters* **2**, 365 (1959). J. Bowcock, W. N. Cottingham, and D. Lurie, *ibid.*, **5**, 386 (1960). Gyo Takeda, *Phys. Rev.* **100**, 440 (1955).

³ F. J. Dyson, *Phys. Rev.* **99**, 1037 (1955); Y. Nambu, *ibid.*, **106**, 1366 (1957); G. F. Chew, *Phys. Rev. Letters* **4**, 142 (1960); J. Sakurai, *Ann. Phys.* **11**, 1 (1960); G. Breit, *Proc. Natl. Acad. Sci. U. S.*, **46**, 746 (1960).

⁴ A. Abashian, N. E. Booth, and K. M. Crowe, *Phys. Rev. Letters* **5**, 258 (1960); E. Pickup, F. Ayer, and E. O. Salant, *ibid.*, **5**, 161 (1960); J. G. Rushbrooke and D. Radojivic, *ibid.*, **5**, 567 (1960); F. Bonsignori, V. Bortolani, and A. Stanghellini, *Nuovo cimento* **18**, 1237 (1960); I. Derado, *ibid.*, **15**, 853 (1960).

⁵ J. Anderson, V. Bang, P. Burke, D. Carmony, and N. Schmitz, *Phys. Rev. Letters* **6**, 365 (1961).

⁶ A. R. Erwin, R. March, W. D. Walker, and E. West, *Phys. Rev. Letters* **6**, 628 (1961).

⁷ D. Stonehill, C. Baltay, H. Courant, W. Fickinger, E. C. Fowler, H. Kraybill, J. Sandweiss, J. Sanford, and H. D. Taft, *Phys. Rev. Letters* **6**, 625 (1961).

⁸ E. Pickup, D. K. Robinson, and E. O. Salant, *Phys. Rev. Letters* **7**, 192 (1961).

⁹ B. C. Maglic, L. W. Alvarez, A. H. Rosenfeld, and M. C. Stevenson, *Phys. Rev. Letters* **7**, 178 (1961).

¹⁰ A. Pevsner, R. Kramer, M. Nussbaum, C. Richardson, P. Schlein, R. Strand, T. Toohig, M. Block, A. Engler, R. Gessaroli, and C. Meltzer, *Phys. Rev. Letters* **7**, 421 (1961).

¹¹ P. L. Bastien, J. P. Berge, O. I. Dahl, M. Ferro-Luzzi, D. H. Miller, J. J. Murray, A. H. Rosenfeld, and M. B. Watson, *Phys. Rev. Letters* **8**, 114 (1962).

¹² R. Barloutaud, J. Heughebaert, A. Leveque, J. Meyer, and R. Omnes, *Phys. Rev. Letters* **8**, 32 (1962); C. Peck, L. Jones, and M. Perl (to be published); B. Sechi Zorn, *Phys. Rev. Letters* **8**, 282 (1962).

TABLE II. Classification of identified π^+p two-prong reactions.

Energy (MeV)	Total Number	Elastic	($p, +, 0$)	($n, +, +$)	Multiple π production
910	2045	944	846	209	46
1090	2520	1205	951	249	115
1260	3868	1745	1365	490	268

tum transfers to the target proton than other interaction mechanisms, and should, therefore, be favored by selecting reactions in which the laboratory momentum of the secondary nucleon is less than about three-pion masses.

The effect of the energy-dependent di-pion interaction at 760 MeV (ρ meson) is shown in Fig. 2, which contains a histogram of the total energy (ω) of

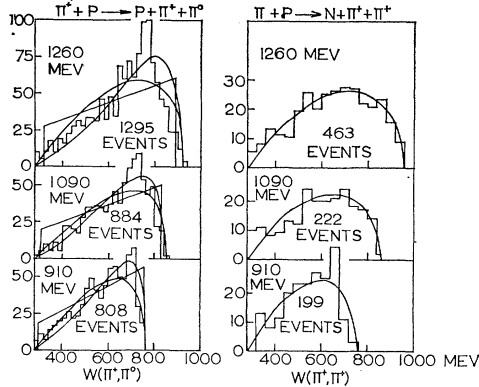


FIG. 2. Total energy W of the two secondary pions in their center of mass, for all reactions $\pi^+ + p \rightarrow p + \pi^+ + \pi^0$ and $\pi^+ + p \rightarrow n + \pi^+ + \pi^+$. (Number of events per 20-MeV interval.)

the π^+ and π_0 secondaries in the reaction $\pi^+ + p \rightarrow p + \pi^+ + \pi^0$. Peaks occur near $\omega = 750$ MeV for the 1090- and 1260-MeV energies. These peaks extend far above the three-body phase space curve, and also above the trapezoidal-like spectrum produced by decay of the nucleon isobar of mass 1230 MeV. Also plotted for comparison, is the asymmetrical curve showing the spectrum calculated for a constant pi-pi cross section from the formula given by Chew and Low¹³ for the diagram of Fig. 1:

$$\frac{\partial^2 \sigma}{\partial \Delta^2 \partial \omega^2} = \frac{f^2}{2\pi} \frac{\Delta^2 / \mu^2}{(\Delta^2 + \mu^2)^3} \frac{\omega}{q^2} (\frac{1}{4}\omega^2 - \mu^2)^{1/2} \sigma(\pi^+ \pi^0).$$

This formula strictly applies only in the limit as one approaches the pole of real pion emission, but was used here throughout the entire physical energy re-

¹³ G. F. Chew and F. E. Low, Phys. Rev. Letters 113, 1640 (1959).

gion. The resulting spectra have maxima which are broader and at different energy from the observed peaks, which also extend significantly above these curves. The peak at 1260 MeV contains 54 events above the curve for constant di-pi cross section, corresponding statistically to 4.5 standard deviations. At 1090 MeV, the peak is 2.5 standard deviations. Selecting events with momentum transfer to the proton of less than 400 MeV/c, reduces the background and enhances the peaks for the energies 1090 and 1260 MeV, as appears in Fig. 3.

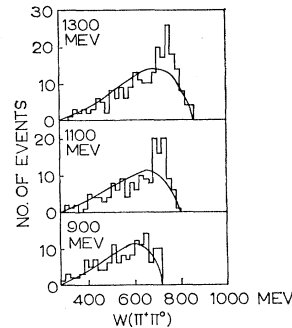


FIG. 3. Total energy W of the two secondary pions in their center of mass, for reactions $\pi^+ + p \rightarrow p + \pi^+ + \pi^0$ in which laboratory momentum of the secondary proton is less than 400 MeV/c.

The I spin of the " ρ " meson is clearly shown by comparison of the ω spectra of events producing $p\pi^+\pi^0$ with those producing $n\pi^+\pi^+$ shown in Fig. 2. The ω spectra for the $n\pi^+\pi^+$ reactions show no significant peaking, and conform well to the three-body phase space curve. This is consistent with a di-pi I spin equal to 1, which does not occur at all in the $n\pi^+\pi^+$ reactions. On the other hand, assuming I spin conservation, I spin 2 is 4 times as frequent in $n\pi^+\pi^+$ events as in $p\pi^+\pi^0$ events, and I spin 0 does not appear in either process. The assignment I spin 1 agrees with our earlier conclusions⁷ and those of other laboratories.

The energy width (Γ) of the di-pi interaction is related to its lifetime (τ) by the well-known relation $\tau \simeq \hbar/\Gamma$. It is therefore desirable to determine the width as precisely as possible. The width which we obtain experimentally, however, depends upon the amount of background which we assume to be present. Selecting low momentum transfers to the nucleon reduces this background but does not eliminate it in π^+p interactions. In these reactions there is a strong production of the nucleon 1230-MeV isobar. Figure 4 clearly shows this; at all three energies there is a pronounced peak at 150 MeV in the π^+ -proton Q -value spectrum. The effect of both the isobar and the meson is shown in Fig. 5, where the total energy in the Center of mass system (c.m.s.) of the π^+ is plotted against the total energy of the π^0 (Dalitz

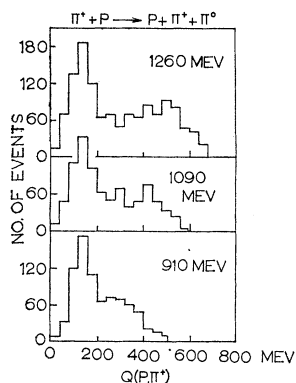


FIG. 4. Kinetic energy Q of the proton and positive pion in their center of mass, for all reactions $\pi^+ + p \rightarrow p + \pi^+ + \pi^0$.

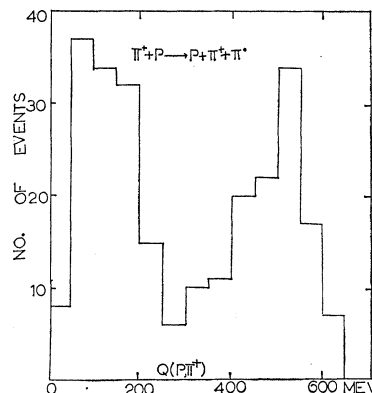


FIG. 6. Kinetic energy of positive pion and proton in their center of mass, for reactions $\pi^+ + p \rightarrow p + \pi^+ + \pi^0$ in which laboratory momentum of secondary-proton is < 400 MeV/c.

plot). The size of each black spot is proportional to the density of events in that area. Ridges of high density are apparent in the di-pi and isobar regions. The region where the di-pi and isobar ridges intersect is of interest, with respect to possible interference between the di-pi and the isobar production. A population density greater than the simple sum of the two

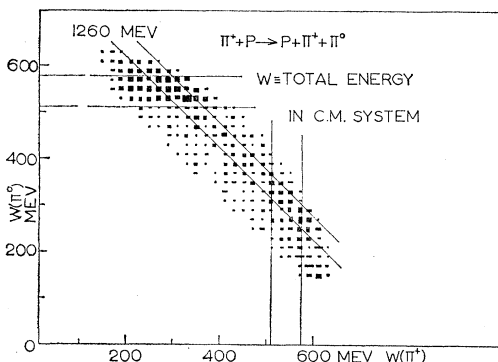


FIG. 5. Density of events in the $w(\pi^+) - w(\pi^0)$ plane for the reaction $\pi^+ + p \rightarrow p + \pi^+ + \pi^0$. $w(\pi)$ is the pion total energy in the system's center of mass. Horizontal lines enclose the region of $\pi^+ - p$ isobar. Vertical lines enclose the region of $\pi^0 - p$ isobar. Slanting lines enclose the " ρ " region.

ridges would indicate strong interference between the two states. This may be present in one of the cells in the intersection, which contains 34 events, whereas the sum of the ridges is 24.

The enhancement of the pi-pi interaction peaks relative to background is shown in Fig. 3, where the ω spectra are plotted for events with secondary-proton momentum less than 400 MeV/c. However, the nucleon 1230-MeV isobar is still present in the final state of these interactions. This is apparent from Fig. 6, where the peak at 150 MeV $\pi^+ - p$ Q value is still pronounced in the events with low momentum transferred to the proton. Figure 7 shows the pi-pi cross section computed from the data of Fig. 3, using the

Chew-Low formula, ignoring the background. The full width at half-maximum of these peaks, obtained from Fig. 7, is 120 MeV. Since the background will tend to increase the apparent width, 120 MeV is an upper limit to the true width, which probably lies between 60 and 120 MeV. *Note added in proof:* We have since attempted to fit the data of Fig. 7 with a single level resonance formula in the $J = 1$ state, combined with an incoherent hard-sphere scattering background in angular momentum states $J = 0$ to $J = 3$. A maximum likelihood procedure yielded the following parameters:

Beam energy	Resonance energy	Resonance full width
1090 MeV	726 ± 10	61 ± 24
1260	755 ± 10	57 ± 27

However, attempts to fit the data with a coherent

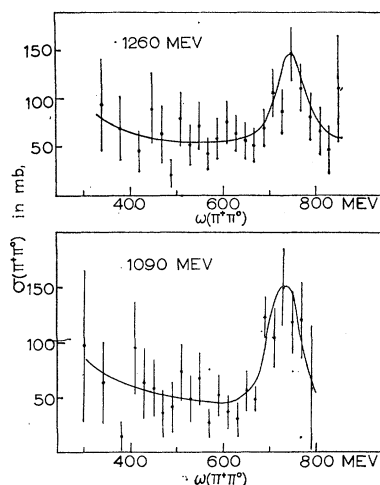


FIG. 7. Pion-pion cross sections, computed by applying Chew-Low formula to reactions $\pi^+ + p \rightarrow p + \pi^+ + \pi^0$ in which laboratory momentum of secondary-proton is less than 400 MeV/c.

background have shown that the fitted parameters are strongly dependent on the assumed model.

The angular momentum of the ρ meson is expected theoretically to be 1. Because the pion is a boson and the I spin is odd, the angular momentum must also be odd. The large energy width and resulting short lifetime of the rho meson precludes a spin of 5 or higher, which would have a long lifetime because of the angular momentum barrier, and tends to make the assignment $J = 1$ somewhat more probable than $J = 3$. Several workers^{8,14} have made studies of the angular distribution of the di-pi decay which are consistent with $J = 1$. The long lifetime of the rho, coupled with the presence of the nucleon 1230-MeV isobar, makes the validity of an Adair-type analysis doubtful in $\pi^+ - p$ interactions. In fact, it is possible for a background as low as 12% to produce isotropy from an expected angular distributions of $1 + 3 \cos^2 \theta$. To test this question, we have tried to determine the spin of the 1230-MeV isobar, which is known to be $3/2$. The results are shown in Fig. 8, where the experimental distribution obtained is vastly different

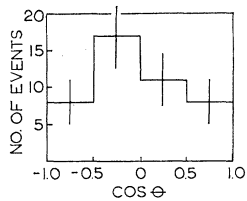


FIG. 8. Angular distribution ($\cos \theta$) of positive pion from decay of 1230-MeV nucleon-isobar, in the reactions $\pi^+ + p \rightarrow p + \pi^+ + \pi^0$ for which $|\cos \theta_p| > 0.9$. θ_p is the angle between the line of flight of the isobar in the c. m. s. and the incident direction. θ is the angle, in the isobar's center of mass, between the positive pion and the incident direction.

from the $1 + 3 \cos^2 \theta$ which the analysis predicts. A more detailed analysis appears to be required, if useful information concerning the di-pi spin is to be extracted by this means.

The maximum value of the $\pi^+\pi^0$ resonant cross section (95 mb) favors $J = 1$ instead of $J = 3$ or higher. In order for this value to be consistent with $J = 3$, the amplitude for all other decay modes of the ρ must be comparable in magnitude to the amplitude for $\rho \rightarrow \pi^+ + \pi^0$. Our search for these other decay modes, $\rho \rightarrow 2\pi^+ + \pi^- + \pi^0$ and $\rho \rightarrow \pi^+ + 3\pi^0$, indicates a total amplitude for these processes of at most 1/6 of the amplitude for decay to $\pi^+ + \pi^0$. This is inconsistent with a spin assignment of $J = 3$ or higher.

We have also searched for the presence of other

¹⁴ D. Carmony and R. T. Van de Walle, Phys. Rev. Letters 8, 73 (1962); Report to the Internationale Conference d'Aix en Provence by the groups at Bari, Bologna, Orsay, and Saclay (unpublished).

pion-pion interactions besides the rho meson. The omega meson is not present since the available energy is barely sufficient to produce it by the reaction $\pi^+ + p \rightarrow p^+ + \omega^0 + \pi^+$. There is weak evidence, however, for the presence of the eta meson, in the

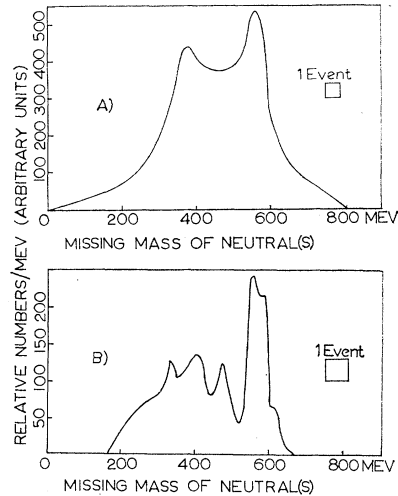


FIG. 9. Ideograms of neutral missing mass for the reactions $\pi^+ + p \rightarrow p + \pi^+ + \text{neutral}(s)$, at 1260-MeV energy: (A) All reactions. (B) Reactions for which laboratory momentum of secondary-proton is below 400 MeV/c.

missing-mass spectrum of the events which produce $\pi^+ + p + \text{neutral}(s)$. This spectrum, shown in the ideograms of Fig. 9, has a peak at 560 MeV, after selection of events with secondary-proton momentum below 400 MeV/c. The peak contains 9 events, compared to an average of 3 events per equal interval on either side of the peak.

The zeta meson, if it exists, is not discernible in these data. It has been reported to appear as a peak in the ω spectrum at about 575 MeV.¹² Reference to Figs. 2 and 3 shows no indication of a peak at this energy in these data. It has been suggested that this interaction may occur with high momentum transfer

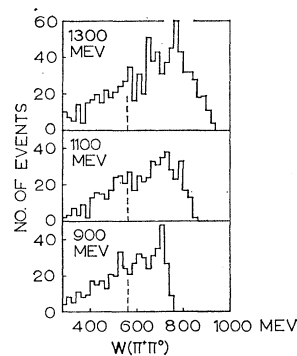


Fig. 10. Total energy W of the two secondary-pions in their center of mass, for reactions $\pi^+ + p \rightarrow p + \pi^+ + \pi^0$ in which laboratory momentum of the secondary-pion is above 550 MeV/c.

to the nucleon. Therefore, we have plotted the ω spectrum for events with momentum of the secondary-proton greater than 550 MeV/c (Fig. 10). The zeta is still not apparent.

We are indebted to the Bubble Chamber Group and the Cosmotron Department of the Brookhaven

National Laboratory, for generous technical assistance in producing the bubble chamber pictures for this study, to the technicians of the Yale high-energy group for scanning the pictures and measuring the interactions, and to the other physicists of the Yale high-energy group for many stimulating discussions.

Approximation Formulas for Nonrelativistic Bremsstrahlung and Average Gaunt Factors for a Maxwellian Electron Gas

P. J. BRUSSAARD*

F.O.M.-Instituut voor Plasmafysica, Jutfaas, Netherlands

AND

H. C. VAN DE HULST

Sterrewacht, Leiden, Netherlands

1. INTRODUCTION

THE radiation emitted during encounters of electrons with ions in a fully ionized gas of low density is called bremsstrahlung. The term "free-free transitions," which is customary in the astrophysical literature, refers to the same process. This radiation has proved to be of importance in cosmic-ray studies, in radio astronomy, in gas discharges, in thermonuclear experiments, and in other physical and astrophysical problems. The wide range in energy and frequency met in these applications necessitates different approximation formulas. This fact, combined with the fact that the relevant literature is spread over a long time interval, from Kramers (1923)¹ to now, makes it difficult to obtain a clear survey of the literature for practical purposes.

The aim of this paper is to collect in a concise manner the most important approximations that permit the rapid calculation of numerical results in the entire energy and frequency ranges with an accuracy of one percent.

The discussion, which can be naturally divided into a part dealing with incoming electrons of one velocity only (Secs. 2-5) and a part dealing with a

gas having a Maxwellian velocity distribution (Secs. 6-9), is limited to nonrelativistic energies, i.e., energies smaller than 10^4 eV or temperatures lower than 10^8 °K, approximately. The restriction to low energies means that the formulas for dipole radiation suffice. Screening effects, arising from penetration of the electron into the electron shell of an atom (for very low energies), have also been omitted [cf., Guggenberger (1957), Hettner (1958)].

Theory and numerical data for bremsstrahlung at higher (relativistic) energies were reviewed by Heitler (1954), J. Stickforth (1961), and in great detail by Koch and Motz (1959). The latter authors state that "The nonrelativistic cross-section formulas derived in the dipole approximation by Sommerfeld with Coulomb wave functions have a complicated form with hypergeometric functions and are difficult to evaluate," and omit from their review a discussion of this topic, which is the exclusive topic of the present paper. Hence, only one formula [their 3 BN(a), our (12)] is common to the two papers.

In Sec. 2, rigorous formulas for electrons of one velocity are reviewed. In Sec. 3, a general division is made of the energy and frequency ranges into regions where different basic assumptions hold. A list of approximation formulas with their domains of validity is given in Sec. 4. In Sec. 5, we discuss the numerical results that are available in the literature.

* Present address: Duke University, Durham, North Carolina.

¹ See the list of references at the end of this paper.